Lasers in Surgery and Medicine 18:72–80 (1996)

Dosimetry Studies Utilizing the Urolase Right-Angle Firing Neodymium:YAG Laser Fiber in the Human Prostate

John N. Kabalin, MD, Martha K. Terris, MD, Maria Laura Mancianti, MD, and Luis F. Fajardo, MD

Urology Section (J.N.K., M.K.T.) and Pathology Service (M.L.M., L.F.F.), Palo Alto Veterans Affairs Medical Center, Palo Alto, California 94304; Departments of Urology (J.N.K., M.K.T.) and Pathology (M.L.M., L.F.F.), Stanford University School of Medicine, Stanford, California 94305

Background and Objective: **Until recently, little or no objective data have been available to support either the choice of power setting or the timing of laser applications to achieve optimal tissue ablation in the human prostate. The objective of this study was to define quantitative dosimetry curves for the Urolase right angle laser fiber in human prostates.**

Study Design Materials and Methods: **Transurethral Neodymium:YAG laser application was performed with the Urolase right-angle laser fiber in adult human prostates prior to planned radical surgery. Depth and volume of prostatic tissue coagulation for single, continuous laser applications were measured at variable power settings from 20 to 60 watts while holding total energy delivery constant. Then, holding the power setting constant at 40 watts, the extent of tissue coagulation was measured for variable treatment times from 60 to 120 seconds.**

Results: **Peak tissue coagulation was observed at 40 watts up to a maximum of 14 mm tissue penetration and 4.23 cc volume coagulated following a single spot laser application. The mean depth of tissue coagulation at 40 watts power setting was 13.5 mm, with a mean volume of tissue coagulation of 3.68 cc. The mean depth of tissue penetration at 40 watts was more than 25% greater than that observed at 60 watts, and the mean volume of tissue coagulation was 190% greater than that observed at 60 watts. As treatment time was increased from 60 to 90 seconds, extent of tissue coagulation increased significantly. However, beyond 90 seconds continuous laser application at 40 watts, a plateau in tissue effects was observed, with minimal increase in tissue coagulation between 90 and 120 seconds. Histologic examination of prostates removed acutely showed heat-induced damage to both stromal and glandular epithelial elements in laser-treated areas. At 1 year, the prostatic urethra was lined with a normal transitional epithelium, and mild periurethral fibrosis with focal squamous metaplasia was seen.**

Conclusion: **Using the Urolase right-angle laser fiber, this study suggests that 40 watts power setting and 90 seconds continuous application time with a Neodymium:YAG laser source represent optimal treatment parameters to maximize prostatic tissue coagulation.** © 1996 Wiley-Liss, Inc.*

Accepted for publication October 24, 1994.

Address reprint requests to John N. Kabalin, M.D., Chief, Urology Section (112C), V.A. Medical Center, 3801 Miranda Avenue, Palo Alto, CA 94304.

Key words: benign prostatic hyperplasia, dose-response relationship, radiation, laser surgery, neodymium:YAG, prostate, prostatectomy, urolase

INTRODUCTION

Subtotal prostatectomy for symptomatic bladder outlet obstruction due to benign prostatic hyperplasia (BPH) in older men is one of the most common operative procedures performed in the United States [1]. Standard surgical techniques, most commonly transurethral electrocautery resection of excess BPH tissue, although effective, are associated with recognized and significant morbidities [2]. In recent years, meaningful attempts have been made to develop laser technology appropriate for the performance of simple or subtotal prostatectomy in the hope that lasers will produce a much lower morbidity profile compared to standard surgical techniques. The first of these purpose-designed laser devices for prostatectomy was the TULIP (Intra-Sonix), an ultrasound-guided system using a Neodymium:YAG laser source to cause coagulation necrosis in the prostate [3,4]. Investigators have shown reasonable efficacy and minimal morbidity associated with this approach [5]. However, the equipment is bulky and awkward to use, and in particular the reliance on ultrasound-guidance is viewed as a disadvantage by many urologists. This device has not yet been approved for use in the United States.

Simpler laser delivery systems that can be used through standard endoscopic equipment under direct vision are now available. The first of these was the Urolase right-angle laser fiber (C.R. Bard) [6–8]. This instrument consists of a standard 600-μm quartz laser transmission fiber to which a distal gold-alloy headpiece with a parabolic reflecting mirror has been affixed. Used with a standard Neodymium:YAG laser source at power settings up to 60 watts, this instrument bends the laser beam at a right angle and disperses it in a crescent with approximately a 30° average arc of divergence. This beam configuration covers a relatively wide area with a relatively low energy density and has been used successfully to produce coagulation necrosis and subsequent prostatic tissue ablation in several series of human patients, with remarkably minimal morbidity observed compared to other surgical approaches [9–15]. The Urolase, along with several other more-or-less dissimilar direct vision, free beam Neodymium:YAG delivery systems, are now available in the United States and are being used to perform prostatectomy.

Unfortunately, until recently little or no objective data have been available to support either the choice of power setting or the timing of laser applications to achieve optimal tissue ablation in the human prostate using the Urolase right-angle laser fiber. Even less information exists for the several competing delivery systems that have subsequently been marketed. We have previously reported, first in vitro in a potato model and then in vivo in a canine prostate model, our efforts carefully to delineate dosimetry curves for tissue ablation with the Urolase delivery system employing a Neodymium:YAG laser source [16]. We now extend these observations to the human prostate in an attempt to define optimal treatment parameters for laser prostatectomy with this delivery system.

MATERIALS AND METHODS

A total of 12 adult men with either peripheral zone prostate cancers (clinical Stage B) or invasive transitional cell carcinoma of the bladder (clinical Stage B), who had already opted for either radical prostatectomy or cystoprostatectomy to treat these malignant conditions, volunteered to participate in this study. Patients with a history of prior prostatic surgery were excluded from participation. Informed consent was obtained according to our institutional human subjects committee protocol. Average patient age was 63 years (range 47–70 years).

Immediately prior to their radical cancer surgery and under the same general anesthetic, patients were placed in dorsal lithotomy position and prepped and draped sterilely as for standard cystoscopy. Cystoscopy was performed using a standard 21 F cystoscope and sterile water irrigation at room temperature. The Urolase right-angle laser fiber was advanced into the prostatic urethra through the working port of the cystoscope under direct vision. A standard Neodymium:YAG laser source capable of continuous output was utilized. Neodymium:YAG irradiation was delivered with the Urolase fiber to a single spot location to one or both prostatic lateral lobes (3 o'clock and/or 9 o'clock) for variable treatment times at variable watts settings as described be-

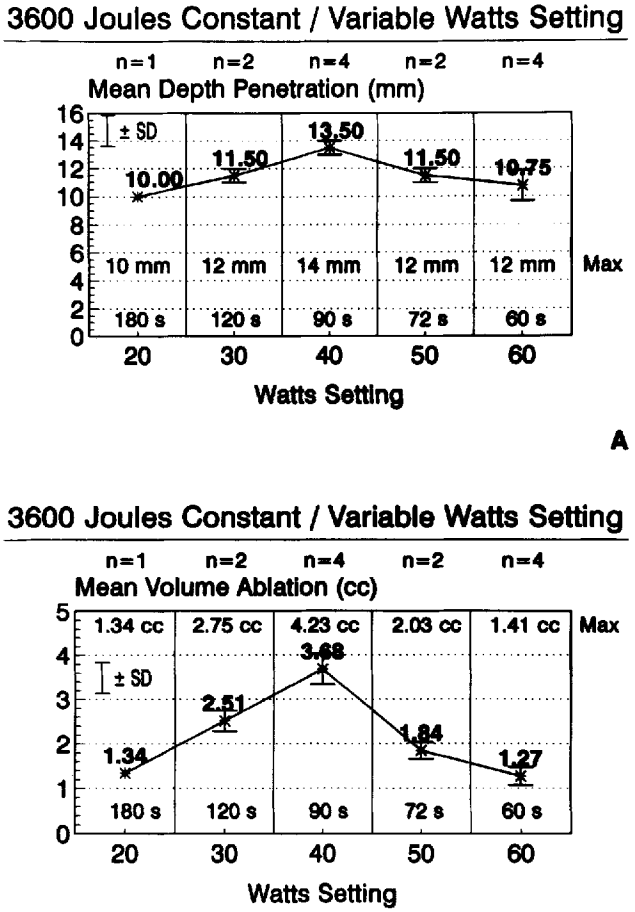

Fig. 1. Dosimetry plots in human prostate for variable power settings from 20 watts through 60 watts, holding total energy delivery constant at 3,600 joules for each setting. Mean values are shown in bold. Error bars represent ± 1 standard deviation. Maximum (Max) values observed for each power setting are also shown, as are total treatment times in seconds (s). **A.** Plot of mean depth of penetration for each power setting in millimeters (mm). **B.** Plot of mean volume of tissue coagulation for each power setting in cubic centimeters (cc).

low. In this fashion, overlap of laser-induced coagulation effects was avoided to allow careful postoperative measurements of each individual laser application site. All laser application times were continuous and without interruption. A new Urolase fiber was used in each case, and thus no more than two laser applications were performed with a single Urolase fiber. Additionally, using an external power meter and testing at 3 watts before and after each application, no degradation in efficiency was observed in any fiber during these brief usages.

Following these brief laser applications, patients were repositioned, reprepped, and re-

TABLE 1. Comparisons of Paired 40-Watt and 60-Watt Laser Applications in Three Prostates, Holding Total Energy Delivery Constant for Each Application at 3,600 Joules*

	Depth comparison	Volume comparison
Pair 1	40w = 29% > 60w	40w = 90% > 60w
Pair 2	40w = 18% > 60w	40w = 206% > 60w
Pair 3	40w = 27% > 60w	40w = 157% > 60w

*In each instance, both the depth and volume of the 40-watt lesion exceeded the 60-watt lesion in the same prostate. The percentage by which the tissue lesion produced by the 40-watt application exceeded that of the 60-watt application in depth and volume for each set of paired tissue lesions in the same prostate is shown.

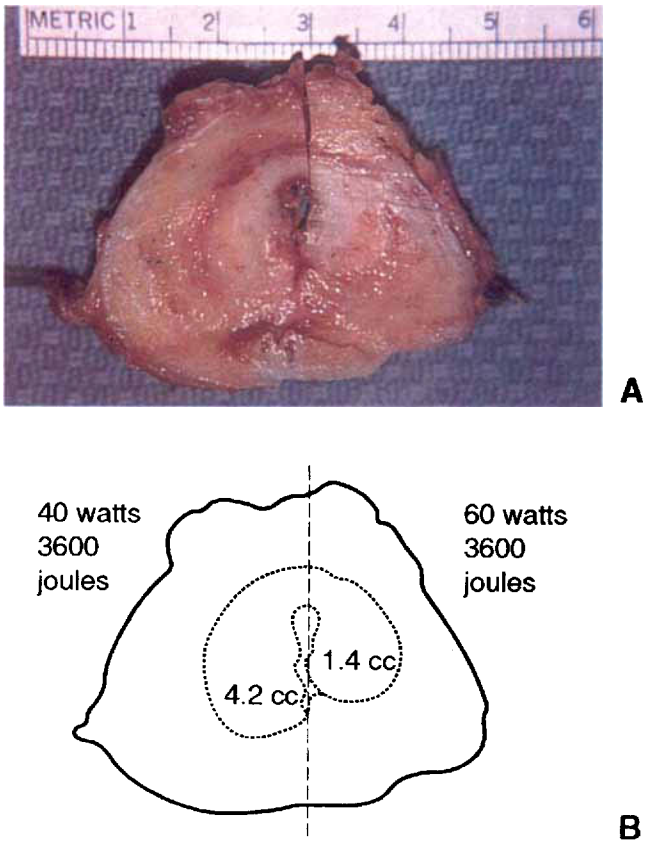

Fig. 2. **A.** Transverse section through human radical prostatectomy specimen following bilateral 3,600 joule lateral lobe Neodymium:YAG laser applications. Pale areas of tissue coagulation in the prostatic transition zone are clearly demarcated. On the left, laser application was continuous at 40 watts for 90 seconds. On the right, laser application was continuous at 60 watts for 60 seconds. The 40-watt application produced a significantly larger volume of tissue coagulation. **B.** Line diagram of section shown in A.

draped, and radical prostatectomy or cystoprostatectomy performed in the usual fashion. No external changes were noticeable in the prostate

or surrounding tissues during open surgery immediately following laser treatment. Prostates were removed surgically 90–120 minutes following laser applications, weighed and fixed overnight in formalin. In cystoprostatectomy cases, the prostate was sharply separated from the bladder specimen before weighing and later examination. Mean prostate weight in this series was 56 g (range 40–90 g). Cystoscopically, excess BPH tissue was estimated on average to be 24 g (range 10–45 g) and prostatic urethral length from bladder neck to veru montanum averaged 2.75 cm (range 2–4 cm).

Prostates were sectioned at 24 hours postoperatively. The area of transition zone coagulation was clearly visible in the gross specimens as a pale or white region. This zone of tissue coagulation produced by each individual laser application was measured in three dimensions, and results are reported both as the absolute depth of the tissue lesion produced and as the volume of the lesion calculated from the above measurements using the formula for a half-ellipsoid ($\pi/6$ · depth · width · length). Standard histologic sections of each prostate, including areas of laser coagulation, were also prepared and stained with hematoxlyin-eosin (H&E) and/or Gomori's trichrome stain. In addition to the examination of acute laser coagulation effects in this series, one additional prostate was obtained from a patient who had undergone Urolase laser prostatectomy 1 year earlier for bladder outlet obstruction and who subsequently developed a small peripheral zone prostate cancer leading to radical prostatectomy. The delayed histologic changes observed in this gland 1 year following laser prostatectomy are also presented.

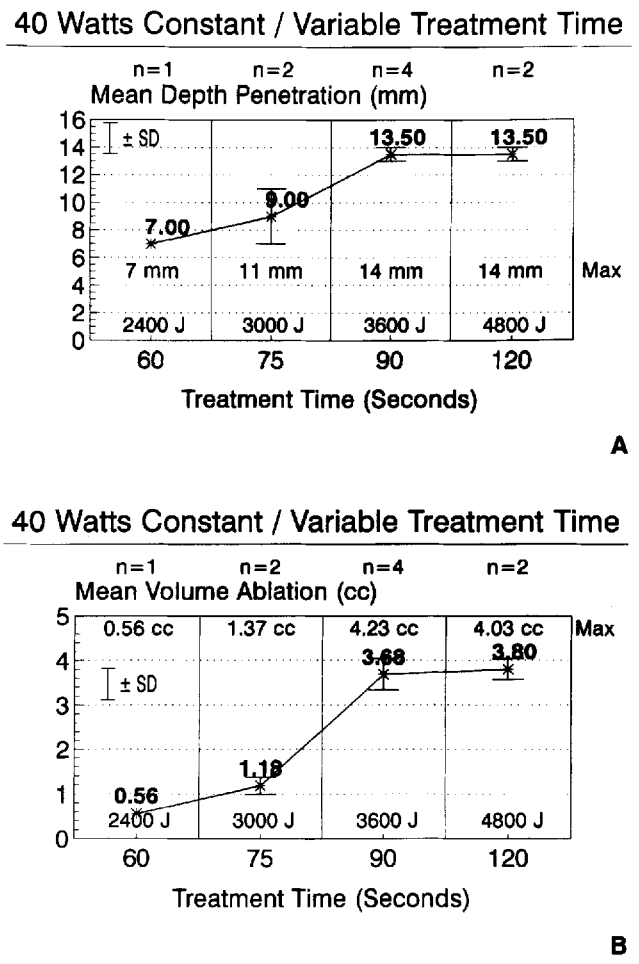

Fig. 3. Dosimetry plots in human prostate for variable treatment times from 60 seconds through 120 seconds, holding the power setting constant at 40 watts. Mean values are shown in bold. Error bars represent ± 1 standard deviation. Maximum (Max) values observed for each treatment time are also shown, as are total energy applications in joules (j). **A.** Plot of mean depth of penetration for each treatment time in millimeters (mm). **B.** Plot of mean volume of tissue coagulation for each treatment time in cubic centimeters (cc).

RESULTS

Effect of Watts Setting

Depth and volume of prostatic tissue ablation for single, continuous laser applications with the Urolase right-angle fiber were measured at variable power settings from 20 to 60 watts while holding total energy delivery constant at 3,600 joules for each setting (Fig. 1). Peak tissue coagulation effects, both in terms of depth of tissue coagulation and total volume of tissue coagulation, were observed at the 40 watts power setting—up to a maximum of 14 mm tissue penetration with a mean of 13.5 mm (Fig. 1A). The mean volume of tissue coagulation at 40 watts was 3.68 cc, with a maximum of 4.23 cc (Fig. 1B).

Despite constant energy delivery, the extent of prostatic coagulation diminished steadily as power settings were lowered through 20 watts. Similarly, the extent of prostatic coagulation decreased significantly as power settings were raised through 60 watts maximum (Figs. 1, 2). The mean depth of tissue coagulation at 40 watts power setting was more than 25% greater than that observed at 60 watts, and the mean volume of tissue coagulation at 40 watts was 190 percent greater than that observed at 60 watts. In three prostates, bilateral laser applications were made at 40 watts to one lateral lobe and at 60 watts to the opposite lateral lobe in a symmetrical fashion.

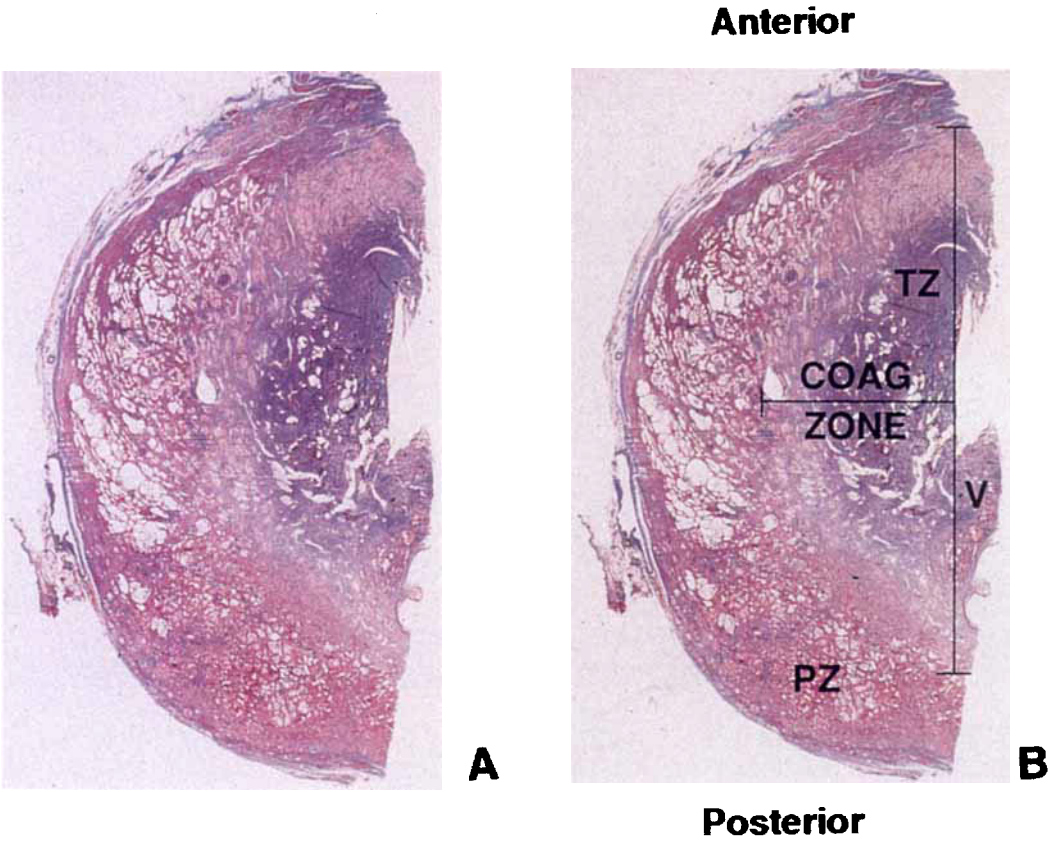

Fig. 4. Acute histologic change following Neodymium:YAG laser coagulation in human prostate. A single laterally directed laser application has been performed with the Urolase. (Gomori's trichrome stain.) **A.** Complete transverse hemisection through prostate with zone of coagulation clearly demarcated by central pale blue region of poor staining (×2). **B.** Same hemisection, with proximal edge of veru montanum (V), prostatic peripheral zone (PZ), prostatic transition zone (TZ), and zone of laser coagulation (COAG ZONE) marked (compare to gross specimen shown in transverse section of Fig. 2A).

The tissue lesion produced by the 40-watt laser application exceeded in both depth and volume the lesion produced by the 60 watt laser application in each of these three paired comparisons (Table 1, Fig. 2), thus affording some control for potential variables in treatment conditions, including but not limited to tissue composition, blood flow, and irrigation characteristics.

Effect of Treatment Time

Holding the power setting constant at 40 watts (a setting observed with the Urolase fiber to produce the most efficient tissue coagulation in human prostates as described above), depth and volume of tissue coagulation were measured for variable treatment times between 60 and 120 seconds (Fig. 3). This implies variable energy delivery at the 40 watts power setting, which ranged from 2,400 joules to 4,800 joules for each laser application. As the time of laser application was increased incrementally from 60 seconds to 90 seconds, the depth and volume of tissue coagulation were observed to increase significantly. However, beyond 90 seconds continuous laser application, a plateau in tissue effects was observed, with no significant increase in tissue coagulation between 90 second and 120 second treatment times.

Histologic Findings in Human Prostates

The area of transition zone laser coagulation was easily distinguishable in the gross specimens as a pale or white region, which was also palpably much firmer than surrounding uncoagulated prostatic parenchyma, and further demarcated by a thin rim of hemorrhage in almost every case (see Fig. 2A). This grossly pale area was shown to correspond histologically to areas of thermal tissue damage, best demonstrated with trichrome stain. The region of thermal injury was easily distinguished by decreased affinity for the trichrome

stain, producing a pale coagulation zone (Fig. 4). Microscopic examination found widespread glandular epithelial disruption in areas of thermal effect (Fig. 5A), characterized by desquamation of the luminal epithelial cell layer. Acute loss of the prostatic glandular basal cell layer was also variably observed. Stromal damage was distinguished histologically by elongation and pyknosis of smooth muscle cell nuclei and by loss of the acid red cytoplasmic staining normally demonstrable in trichrome stained sections (Fig. 5B,C). Prostatic parenchymal muscle fibers appear especially susceptible to the thermal injury caused during laser prostatectomy.

Examination of the prostate obtained at radical prostatectomy 1 year following Urolase laser prostatectomy revealed a 2 × 3 cm prostatectomy defect produced by laser ablation (Fig. 6). This defect had been completely re-epithelialized with an essentially normal transitional cell epithelium lining the prostatic urethra (Fig. 7A). Mild periurethral fibrosis was present, extending 2–3 mm beneath the transitional epithelium. Although most prostatic glandular elements in the transition zone were normal, occasional foci of squamous metaplasia were noted in periurethral areas (Fig. 7B).

DISCUSSION

Initial human clinical trials have demonstrated the safety and efficacy of laser prostatectomy performed with the Urolase right-angle laser fiber [9–15]. We are now actively engaged in efforts to maximize the efficacy of laser ablation of the prostate for the treatment of BPH. For these efforts to prove successful, a better understanding is needed of the tissue effects produced in the human prostate by low energy density, long duration Neodymium:YAG laser applications utilizing instrumentation such as the Urolase fiber. The present study provides important information contributing to our understanding of these tissue effects.

The histologic changes seen here document the acute thermal injury produced in the human prostate during laser prostatectomy. These histologic findings are neither specific to source (laser) nor organ (prostate), but rather are characteristic of heat-induced tissue injury [17]. During free-beam laser coagulation prostatectomy as described, most of the transmitted laser energy is converted to heat and tissue necrosis as a result of thermal injury is the cause of bulk tissue loss over the long term. The findings 1 year after laser prostatectomy show complete healing of the prostatic urethra with few histologic changes occurring in the residual normal transition zone, including mild periurethral fibrosis (no more than 2–3 mm in depth) and occasional foci of squamous metaplasia in periurethral prostatic glandular elements.

The extent of heat-induced tissue damage occurring during laser prostatectomy is not directly proportional to laser power setting. In general, lower or more moderate laser power settings (e.g., 40 watts) produce significantly greater prostatic tissue effects than very high power settings (e.g., 60 watts). At high power settings—which translate to higher rates of energy delivery—tissue surface effects including searing and charring are magnified. This decreases laser light transmission into tissue, absorption of thermal energy by the prostate, and subsequent heat conduction through prostatic tissue to produce the desired effects of deep prostatic coagulation with necrosis. There also appears to be a low end threshold effect in the rate of energy delivery, such that tissue effects are again observed to diminish significantly at very low power settings (e.g., 20 watts). At these lower rates of energy delivery (below 40 watts using the Urolase fiber in this study), the dissipation of thermal energy by the constant flow of cool irrigant through the prostatic urethra during transurethral surgery and also by tissue blood flow limits the ability to heat prostatic tissue to lethal temperatures. In other words, given the low rate of heat production in tissue during these low power laser applications, heat is drawn away from the treated tissues fast enough to prevent tissue damage beyond a certain radius from the spot of laser application, effectively limiting both the depth and total volume of prostatic tissue undergoing coagulation and necrosis.

With prolonged laser application times, a plateau effect is observed with regard to extent of prostatic tissue coagulation. Holding the power setting constant at 40 watts and incrementally increasing treatment times from 60 seconds to 90 seconds, a steady increase in tissue effects was observed. However, beyond 90 seconds this dosimetry curve levels off relatively rapidly, with minimal increase in tissue effects through 120 seconds, i.e., diminishing returns for increasing time and energy delivery beyond a certain threshold level (see Fig. 3). Ongoing energy delivery beyond approximately 90 seconds fails to significantly increase the depth or volume of tissue coagulation

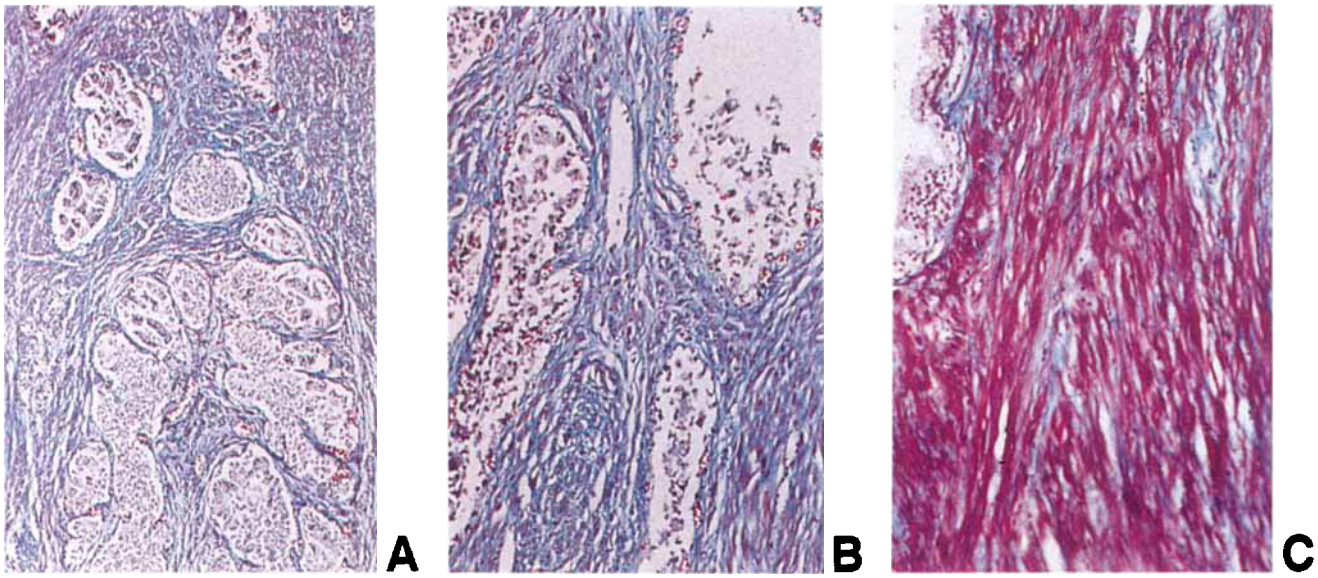

Fig. 5. Acute histologic changes following Neodymium:YAG laser coagulation in human prostate. (Gomori's trichrome stain.) **A.** Region of laser-induced thermal injury, demonstrating desquamation of prostatic glandular epithelium and stromal smooth muscle disruption (×50). **B.** Higher magnification showing region of laser treatment with loss of acid red stain from stromal smooth muscle as a result of thermal injury (×100). **C.** For comparison, nontreated normal prostate with intact stromal smooth muscle (bright red stain) and epithelial elements (×100).

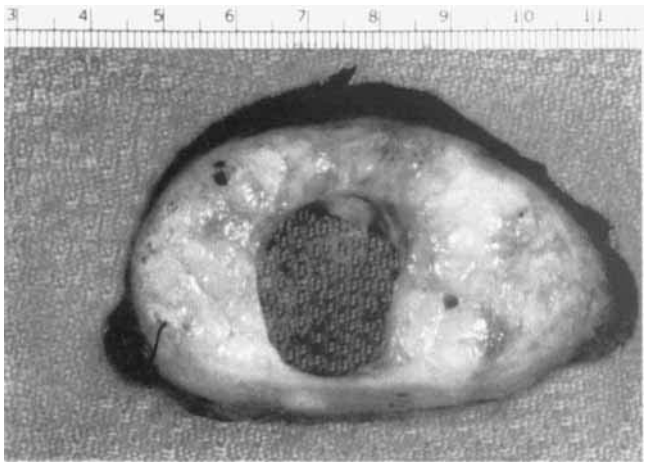

Fig. 6. Transverse section through radical prostatectomy specimen 1 year following laser prostatectomy. Prostatectomy defect (2 × 3 cm) is present and prostatic urethra is smooth and completely re-epithelialized.

in the human prostate. This plateau effect essentially places a physical limit on the depth and extent of tissue injury during such low energy density, prolonged Neodymium:YAG laser applications. Whereas this limitation may restrict therapeutic efficacy in a small subset of men with the largest prostates, in general, this observation probably largely accounts for the remarkable safety of this technology that has been observed in clinical trials. Even in very small prostates, it may be relatively impossible to perforate the gland and cause injury to surrounding tissues, and certainly no such injury has yet been reported.

Such observations also imply that a significant portion of the tissue injury produced by these low energy density, prolonged duration Neodymium:YAG laser applications is not a direct laser effect but an indirect process. A certain threshold energy absorption by the treated tissue must occur within the range of penetration of the Neodymium:YAG laser beam, beyond which further laser energy application results in increasing thermal energy conduction and injury to surrounding tissues—an indirect or secondary injury that may far exceed the direct tissue penetration of the Neodymium:YAG light. The plateau effect seen with prolonged laser application times would not be expected if all tissue injury were a result of direct laser effects. This plateau, however, is predicted if a major portion of the tissue effect observed is due to indirect heat conduction through tissues not directly impacted by the Neodymium:YAG beam, with a finite destructive range before significant dissipation of the heat by an increasingly larger ellipsoidal surface area of cooler tissue and fluid medium.

Using the Urolase right-angle laser fiber, this study suggests that 40 watts power setting

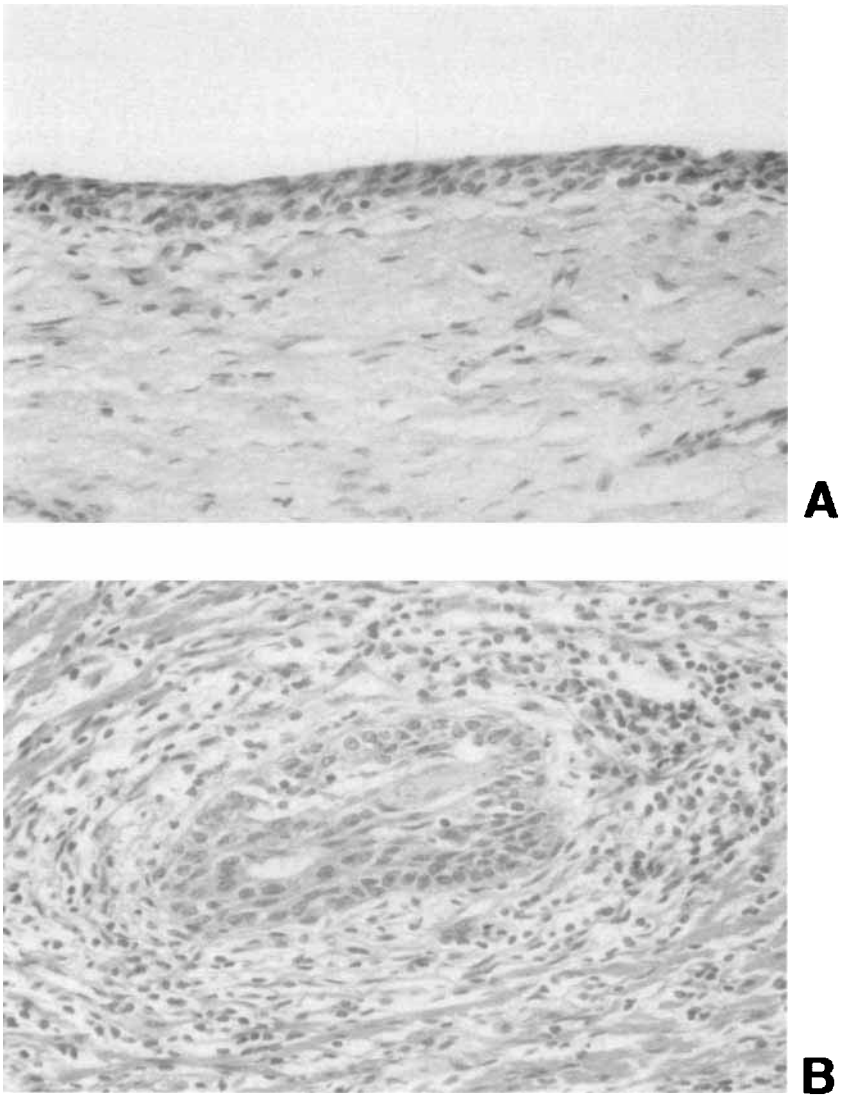

Fig. 7. Histologic findings in human prostate 1 year following laser prostatectomy (same prostate shown in Fig. 6), standard H&E stain (×200). **A.** Prostatic urethra is completely re-epithelialized with normal transitional cell lining. There is approximately a 2–3 mm zone of subepithelial fibrotic change. **B.** Prostatic glands are generally normal, with occasional squamous metaplasia in periurethral areas as shown here.

and 90 seconds continuous application time with a Neodymium:YAG laser source represent optimal treatment parameters to maximize prostatic tissue coagulation. The mean depth of tissue penetration and mean volume of tissue coagulation at the midrange 40 watts power setting are observed to be markedly superior to results achieved at either lower or higher power settings, holding total energy delivery constant (see Figs. 1,2). This is of particular clinical interest, since following initial successes with this device at 40 watts power setting [10,11], the assumption was made that if 40 watts was good, even higher power settings must be better at tissue removal, and a large number of patients have subsequently received 60-watt laser treatments [12,13]. Prior laboratory studies [16] now confirmed by the present work provide compelling evidence against the use of these higher power settings, since they are observed actually to produce much less efficient prostatic coagulation with the Urolase delivery system.

The data provided by this study add to our general understanding of thermal injury in the human prostate produced by long duration, low

energy density Neodymium:YAG laser application and provide specific guidelines for laser prostatectomy performed with the Urolase right-angle laser fiber. However, although the general principles delineated herein will be applicable, specifics such as exact power settings and laser application times may vary with other free-beam Neodymium:YAG delivery systems now available for urologic surgical use. Each of these new delivery systems produces a laser beam with a different physical configuration. Depending upon the delivery fiber, the arc of beam divergence varies from ~ 15–35°, the incident angle of the beam varies over an even wider range, and the energy density of the resultant laser beam varies considerably. Unique dosimetry curves can be predicted and expected to exist for each unique beam configuration produced by each delivery system. Thus the 40-watt power setting and 90-second application time specified here as optimal parameters for the Urolase fiber cannot be generalized to other systems, and there will be a need and demand for careful tissue dosimetry studies for each of the dissimilar laser beam configurations produced by present-day and future laser fibers.

ACKNOWLEDGMENTS

This study supported by a grant from the Providence Foundation.

REFERENCES

1. Holtgrewe HL, Mebust WK, Dowd JB, Cockett ATK, Peters PC, Proctor C. Transurethral prostatectomy: Practice aspects of the dominant operation in American urology. J Urol 1989; 141:248–253.
2. Mebust WK, Holtgrewe HL, Cockett ATK, Peters PC, Writing Committee. Transurethral prostatectomy: Immediate and postoperative complications: A cooperative study of 13 participating institutions evaluating 3,885 patients. J Urol 1989; 141:243–247.
3. Assimos DG, McCullough DL, Woodruff RD, Harrison LH, Hart LJ, Li W-J. Canine transurethral laser-induced prostatectomy. J Endourol 1991; 5:145–149.
4. Roth RA, Aretz HT. Transurethral ultrasound-guided laser-induced prostatectomy (TULIP procedure): A canine prostate feasibility study. J Urol 1991; 146:1128–1135.
5. McCullough DL, Roth RA, Babayan RK, Gordon JO, Reese JH, Crawford ED, Fuselier HA, Smith JA, Murchison RJ, Kaye KW. Transurethral ultrasound-guided laser-induced prostatectomy: National human cooperative study results. J Urol 1993; 150:1607–1611.
6. Johnson DE, Levinson AK, Greskovich FJ, Cromeens DM, Ro JY, Costello AJ, Wishnow KI. Transurethral laser prostatectomy using a right-angle delivery system. SPIE Proceedings 1991; 1421:36–41.
7. Johnson DE, Price RE, Cromeens DM. Pathologic changes occurring in the prostate following transurethral laser prostatectomy. Lasers Surg Med 1992; 12:254–263.
8. Costello AJ, Johnson DE, Bolton CM. Nd:YAG laser ablation of the prostate as a treatment for benign prostatic hypertrophy. Lasers Surg Med 1992; 12:121–124.
9. Costello AJ, Bowsher WG, Bolton DM, Braslis KG, Burt J. Laser ablation of the prostate in patients with benign prostatic hypertrophy. Br J Urol 1992; 69:603–608.
10. Cowles RS, Childs S, Dixon C, Kabalin JN, Lepor H, Stein B, Zabbo A. Prospective randomized study comparing transurethral resection of the prostate to visual laser ablation of the prostate. J Urol 1993; 149:467A.
11. Kabalin JN. Laser prostatectomy performed with a right angle firing Neodymium:YAG laser fiber at 40 watts power setting. J Urol 1993; 150:95–99.
12. Norris JP, Norris DM, Lee RD, Rubenstein MA. Visual laser ablation of the prostate: Clinical experience in 108 patients. J Urol 1993; 150:1612–1614.
13. Kabalin JN, Gill HS, Bite G. Laser prostatectomy performed with a right angle firing Neodymium:YAG laser fiber at 60 watts power setting. J Urol 1995; 153:1502–1505.
14. Kabalin JN, Gill HS. Urolase laser prostatectomy in patients on warfarin anticoagulation: A safe treatment alternative for bladder outlet obstruction. Urology 1993; 42:738–740.
15. Bolton DM, Costello AJ. Management of benign prostatic hyperplasia by transurethral laser ablation in patients treated with warfarin anticoagulation. J Urol 1994; 151: 79–81.
16. Kabalin JN, Gill HS. Dosimetry studies utilizing the Urolase right angle firing Neodymium:YAG laser fiber. Lasers Surg Med 1994; 14:145–154.
17. Fajardo LF, Pathologic effects of hyperthermia in normal tissues. Cancer Res 1984; 44:4826s–4835s.